An Analysis of water hammer pipe flow with unsteady friction model using the SPH Method

Pamplona, A. J. V. P. S.[1], Fernandes Júnior, J.[2], Vasco, J. R. G.[2], Nascimento, A. A.[1]

[1]*Dept. of Mechanical Engineering, Federal University of Goiás*
Av. Esperança, S/N, 74690-900, Goiânia-Goiás, Brazil
almeriopamplona@gmail.com, aanascimento@ufg.br
[2]*Dept. of Hydraulics, Federal University of Goiás*
Av. Universitára, 1488, 74605-220, Goiânia-Goiás, Brazil
jfslmb@gmail.com, joelvasco@ufg.br

Abstract. Two methods used for simulating flow problems in engineering are Method of Characteristics (MOC) and Smoothed Particle Hydrodynamics (SPH). This paper compares the results obtained using these two methods for hydraulic transient in forced conduits. Both steady and unsteady friction losses are considered using the unsteady model proposed by Vardy et al. [1]. The study findings obtained by in-house codes are compared with the experimental results of Martins et al. [2].

Keywords: Smoothed Particles Hydrodynamics, Water Hammer, Unsteady Friction.

1 Introduction

Fluid flow systems rely on effective management of hydraulic transient to ensure system integrity and optimal design. This study investigates this issue using two numerical methods: Smoothed Particle Hydrodynamics (SPH) and the Method of Characteristics (MOC), both coupled with an unsteady friction model.

The SPH method divides the fluid domain into particles that model fluid behavior by computing interactions between them. On the other hand, MOC [3-6] solves partial differential equations (PDEs) that describe fluid behavior in piping or channel systems by tracing flow characteristics to compute changes in flow variables over time.

The SPH method employs the Corrected Smoothed Particle Hydrodynamics (CSPH) method proposed by Chen et al. [7] and artificial viscosity introduced by Monaghan and Gingold [8] to mitigate numerical instabilities arising from shocks and discontinuities.

The simulations incorporate the unsteady friction model proposed by Vardy et al. [1] to consider friction effects on the water hammer phenomenon. This model captures time-dependent frictional forces in the system, providing a more realistic representation of the hydraulic transient. By integrating this model with the SPH method in an in-house code, the study aims to improve the accuracy and reliability of hydraulic transient simulations.

The study compares the SPH and MOC methods to the Martins et al. [2] experiment, obtaining good agreement. The accuracy of the SPH-based simulation is evaluated by assessing the pressure at specific points within the flow during the hydraulic transient phenomenon.

2 Mathematical Models

2.1 Governing Equations

The continuity and momentum equations for a transient flow in one-dimensional pipes are defined as

$$\frac{DH}{Dt} + \frac{c^2}{g}\frac{\partial U}{\partial x} = 0, \tag{1}$$

$$\frac{DU}{Dt} + g\frac{\partial H}{\partial x} + \frac{4\tau}{\rho d} = 0, \tag{2}$$

where H is the manometric height (m), U is the flow mean velocity (m/s), c is the sonic wave speed (m/s), g is the gravitational acceleration (m/s²), τ is the sheer stress on the inner pipe's wall, ρ is the fluid's density (kg/m³), d is the internal pipe diameter, x and t denote the axial distance along the pipe and the time, respectively, D/Dt and $\partial/\partial x$ are the total and the partial derivatives, respectively.

2.2 Unsteady Friction Model

The mathematical model of unsteady friction proposed by Vardy et al. [1] approximates the model derived by Zielke [9] in 1968. The model consists of

$$\tau = \frac{1}{8}\rho\,\lambda\,|U|\,U + \frac{4\,\upsilon\,\rho}{d}[Y_1(t) + Y_2(t)], \tag{3}$$

where υ is the kinematic viscosity (m²/s) and λ is the steady friction (-), approximated by

$$\lambda = \left\{\left(\frac{64}{\Re}\right)^8 + 9.5\left[\ln\left(\frac{\epsilon}{3.7d} + \frac{5.74}{\Re\,0.9}\right) - \left(\frac{2500}{\Re}\right)^6\right]^{-16}\right\}^{\frac{1}{8}}, \tag{4}$$

where $\Re$ is the Reynolds number, and ϵ is the inner pipe wall roughness (m). Futhermore, each Y_m is defined by

$$Y_m(t) = \begin{cases} 0, & t = 0. \\ Y_{m,t-1}\exp\left(-\dfrac{4\,\upsilon\,B_m}{d^2}(t - t^*)\right) + T_m\left(U^t - U^{t^*}\right), & t > 0, \end{cases} \tag{5}$$

where B_m and T_m are constant coefficients, U^t and U^{t^*} are the flow mean velocities in the current instant, and in the immediate anterior instant, respectively. In the work of Vardy et al. [1], the authors presented pre-calculated values of B_m and T_m for several ranges defined by $\lambda_R\,\Re = 0.250\,\lambda\,\Re$, Tab. 1.

Table 1. Values of the coefficients B_m and T_m for several ranges defined by $\lambda_R\,\Re$.

$\lambda_R\,\Re$	T_1	T_2	B_1	B_2
250.000	250.000	74.000	4.400×10^5	4.200×10^5
500.000	260.000	65.000	5.600×10^5	1.150×10^5
1000.000	350.000	65.000	9.800×10^5	4.120×10^5
2000.000	470.000	65.000	2.800×10^5	1.620×10^5

3 The SPH Method

The SPH method consists of an integral convolution approximation of a function f on a domain Ω, using a kernel function,

$$\langle f(x)\rangle = \int_\Omega f(x')W(|x - x'|, h)\,\mathrm{d}x', \tag{6}$$

where $\langle\cdot\rangle$ is the approximation operator, h is the smoothing length, and W is the smoothing or kernel function. The gradient operator application on eq. (6) leads to the derivative approximation of f. Considering the kernel function a Dirac function approximation, the integral on the support domain boundaries becomes null. As a result, the derivative approximation of f is

$$\left\langle\frac{\partial f(x)}{\partial x}\right\rangle = \int_\Omega [f(x') - f(x)]\frac{\partial W(|x - x'|, h)}{\partial x}\mathrm{d}x', \tag{7}$$

Then, the domain is divided into particles with defined physical properties such as mass and density. That allows a particle representation of eqs. (6) and (7) as

$$\langle f(x_i)\rangle = \sum_{j=1}^{n_i} f(x_j)\, W_{ij} \frac{m_j}{\rho_j}, \tag{8}$$

$$\langle \frac{\partial f(x_i)}{\partial x}\rangle = \sum_{j=1}^{n_i} \left[f(x_j) - f(x_i)\right] \frac{\partial W_{ij}}{\partial x} \frac{m_j}{\rho_j}, \tag{9}$$

where the infinitesimal volume element $\mathrm{d}x'$ becomes m_j/ρ_j, with m_j and ρ_j being the mass and the density of the jth particle within the ith particle neighborhood. Moreover, n_i is the total neighbors of the ith particle, W_{ij} is the kernel applied on $|x_i - x_j|$, and $\partial W_{ij}/\partial x$ is the kernel gradient.

3.1 Smoothing function and boundary treatment

The smoothing function is an even function that depends on the distribution of the particles within its support domain to approximate a function f accurately. In the current paper, the authors used the cubic spline function defined by Monaghan and Lattanzio [10] as

$$W(s,h) = \frac{1}{6h}\begin{cases} (2-s)^3 - 4\,(1-s)^3, & 0 \le s < 1, \\ (2-s)^3, & 1 \le s < 2, \\ 0, & \text{otherwise}, \end{cases} \tag{10}$$

where $s = |x_i - x_j|/h$. The relationship between the kernel accuracy and the particles' distribution is within the capability of the convolution integral with the kernel to represent a polynomial field exactly. This measure capability is called as consistency. Thus, the constant consistency is related to a constant field function by

$$\sum_{j=1}^{n_i} W_{ij} \frac{m_j}{\rho_j} = 1, \tag{11}$$

while the linear consistency is given by

$$\sum_{j=1}^{n_i} (x_i - x_j) W_{ij} \frac{m_j}{\rho_j} = 0, \tag{12}$$

According to eqs. (11) and (12), the accuracy decreases near the support domain boundary due to a lack of particles to maintain constant and linear consistency Therefore, the CSPH method [7], which consists of a Taylor series expansion of $f(x')$ and $\partial f(x')/\partial x$ around a particle at x, neglecting the high-order derivatives and considering the linear consistency to hold. As a result, the eqs. (8) and (9) are rewritten as

$$\langle f(x_i)\rangle = \frac{\sum_{j=1}^{n_i} f(x_j) W_{ij} \frac{m_j}{\rho_j}}{\sum_{j=1}^{n_i} W_{ij} \frac{m_j}{\rho_j}}, \tag{13}$$

and

$$\langle \frac{\partial f(x_i)}{\partial x}\rangle = \frac{\sum_{j=1}^{n_i} \left[f(x_j) - f(x_i)\right] \frac{\partial W_{ij}}{\partial x_{ij}} \frac{m_j}{\rho_j}}{\sum_{j=1}^{n_i} (x_i - x_j) \frac{\partial W_{ij}}{\partial x_{ij}} \frac{m_j}{\rho_j}}, \tag{14}$$

3.2 Artificial Viscosity

The SPH method represents spurious numerical oscillations and particle non-physical interpenetration when used to simulate phenomena that have shock waves. To mitigate these aspects, Monaghan [11] added a dissipative term to the momentum equation. The term is known as artificial viscosity and has the following form:

$$\Pi_{ij} = \begin{cases} \dfrac{\beta\, \zeta_{ij}^2 - \alpha\, c\, \zeta_{ij}}{\rho}, & U_{ij} x_{ij} < 0, \\ 0, & \text{otherwise}, \end{cases} \tag{15}$$

where α behaves as a bulk viscosity, β regulates the particles' interpenetration, $U_{ij} = U(x_i, t) - U(x_j, t)$, $x_{ij} = x_i - x_j$, and ζ_{ij} is defined as

$$\zeta_{ij} = \frac{h}{x_{ij}^2} U_{ij} x_{ij}. \tag{16}$$

Hence, the eq. (1) and (2) assume the following discretized form:

$$\left\langle \frac{DH(x_i,t)}{Dt} \right\rangle = -\frac{c^2}{g} \frac{\sum_{j=1}^{n_i} \left[U(x_j,t) - U(x_i,t)\right] \frac{\partial W_{ij}}{\partial x_{ij}} \frac{m_j}{\rho_j}}{\sum_{j=1}^{n_i} (x_i - x_j) \frac{\partial W_{ij}}{\partial x_{ij}} \frac{m_j}{\rho_j}}, \tag{17}$$

and

$$\left\langle \frac{DU(x_i.t)}{Dt} \right\rangle = -g \frac{\sum_{j=1}^{n_i} \left[H(x_j,t) - H(x_i,t)\right] \frac{\partial W_{ij}}{\partial x_{ij}} \frac{m_j}{\rho_j}}{\sum_{j=1}^{n_i} (x_i - x_j) \frac{\partial W_{ij}}{\partial x_{ij}} \frac{m_j}{\rho_j}} - \frac{4 \langle \tau(x_i,t) \rangle}{\rho\, d} - \sum_{j=1}^{n_i} \Pi_{ij} \frac{\partial W_{ij}}{\partial x_{ij}} m_j, \tag{18}$$

where $\langle \tau_i \rangle$ is the unsteady shear stress calculated for the ith path using eq. Then, we calculate the velocity and the manometric height time derivatives at each time step using eq. (17) and and integrate them in time with the Euler method.

4 Error measurement

The current work used the L_2-norm metric to calculate error values. The metric is defined as

$$L_2 = \sqrt{\frac{\sum_{j=1}^{T} \left(f(t_j) - \langle f(t_j) \rangle\right)^2}{\sum_{j=1}^{T} f(t_j)^2}}, \tag{19}$$

where L_2 is the relative error value, $f(t_j)$ is the experimental value, $\langle f(t_j) \rangle$ is the numerical value, and T is the total number of time steps.

5 Experimental and numerical setup

The physical problem consists of a reservoir with a constant pressure head of H_R, a tube with a length of 15.220 m and a diameter of 0.020 m, and a downstream valve. The pipe's roughness measures 1 mm, and it contains water with a density of 1000 kg/m³ and a kinematic viscosity of 1.040×10^{-6} m²/s. The experiment employed a gravity acceleration of 9.806 m/s² and a sonic wave speed of 1250 m/s.

Figure 1 shows a 1D reservoir using the SPH method: h denotes the smoothing length, Δx is the distance between particles' centers, and W represents the smoothing function. The black particle is where the kernel function is applied, and its neighboring particles are the two preceding and two succeeding particles within the compact domain. The pressure at the tube upstream is set as the reservoir's constant pressure. A maneuver equation models a valve downstream.

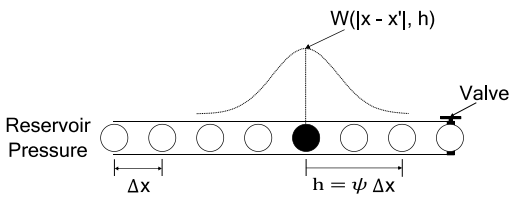

Figure 1. Reservoir-pipe-valve system 1D scheme filled with particles along the x-axis.

The system is similar to the one used by Martins et al. [2]. Thus, the first test was set with $Q_0 = 0.717 \times 10^{-4}$ m³/s, $\Re_0 = 4540$ and $H_R = 46.140$ m; while the second experiment has $Q_0 = 0.961 \times 10^{-4}$ m³/s, $\Re_0 = 6089$ and $H_R = 45.360$ m. Furthermore, the current study employed the valve maneuver modeled by Martins et al. [2]. They use the following relationship between the discharge, Q_v, and the pressure head, H_v, at the downstream end section of the pipe:

$$Q_v = \xi\, Q_0 \sqrt{\frac{H_v}{H_R}}, \tag{20}$$

where ξ is the percentage of the valve opening state, with $\xi = 1$ being a completely open valve and $\xi = 0$ represents a complete close valve. Martins et al. [2] used a hyperbolic model,

$$\xi = 1 - \left(\frac{t - t_i}{t_c - t_i}\right)^8, \tag{21}$$

in their work, where t_i, is the initial time of the closure; and t_c is the closure time. The closure process dour 0.034 s, initializing at 0.269 s and ending at 0.303 s. Moreover, there are 0.269 s of steady-state flow before closing the valve, and the simulation has a total of 1.000 s with 62875-time steps. The final input values to run the simulation are the spatial step, $\Delta x = 0.020$ m, the particles mass, $m_j = \rho_j\, \Delta x\, \Delta y\, \Delta z = (1000$ kg/m³$)(0.020$ m$)(1$ m$)(1$ m$) = 20$ kg, the artificial viscosity variables, $\alpha = 2.000$ and $\beta = 0.000$, and the smoothing length, h = $\psi\, \Delta x = (1.400)(0.020$ m$) = 0.028$ m. Additionally, the Courant-Friedrichs-Lewy number (CFL) is 0.994.

6 Results and discussion

Figure 2 shows the pressure head in the valve with the following parameters: (a) with $Q_0 = 0.717 \times 10^{-4}$ m and $H_R = 46.140$ m, and (b) with $Q_0 = 0.961 \times 10^{-4}$ m³/s and $H_R = 45.360$ m. Between 0.269 s and 0.794 s, both the SPH and MOC methods aligned with experimental results, depicting the pressure wave amplitude and frequency reduction. Furthermore, the numerical wave shape changed from a squarish form to a sinusoidal form, matching the experimental outcome.

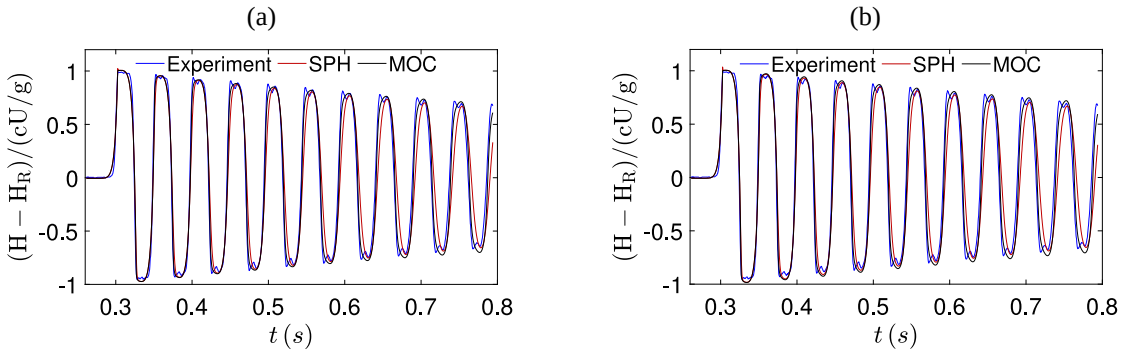

Figure 2. Dimensionless experimental, in blue, and numerical results. (a) $Q_0 = 0.717 \times 10^{-4}$ m and $H_R = 46.140$ m, and (b) $Q_0 = 0.961 \times 10^{-4}$ m³/s and $H_R = 45.360$ m.

There is an error in the valve maneuver model, causing the numerical results to show an early pressure rise. The SPH method shows a non-physical overshoot in the first wave peak, which was fixed by pre-smoothing it using the smoothing features of the CSPH function approximation in eq. (13) [12]. That was done on the velocity distribution in the first seven-time steps after commencing the valve maneuver, two steps before valve closure, and seven steps after valve closure. The pre-smoothed CSPH results are in Fig. 4a, where the overshoot is reduced, but there is still an offset phase difference. This phase difference is also in Fig. 2, which increases over time. Both methods have an offset phase, but it is more pronounced in the SPH method.

The SPH method had an error value almost twice as large as the MOC method's error value, with values of 0.330 and 0.146, respectively, after analyzing the data with Eq. (19). No significant increase in error was observed

for pre-smoothed data, but a slight offset increase was noted compared to the experimental results in Figs. 2 and 4a.

In Fig. 3a there is a smearing effect in the SPH simulation. That could be due to the particles' number, controlled by the Δx value. The first peak and period of pressure history were predicted accurately, but subsequent peaks were not as precise. Increasing the number of particles can reduce the smearing effect. A study found that 762 particles or $\Delta x = 0.02$ m can produce satisfactory results. Qualitative results for any Δx value were not significantly affected by the number of cells in the MOC method. However, the L_2 error for the MOC method remained at 0.146 for $\Delta x \leq 0.020$ m, but increased to 0.189 for $\Delta x \geq 0.040$ m due to a slight shift in the last four peaks in Fig. 3b.

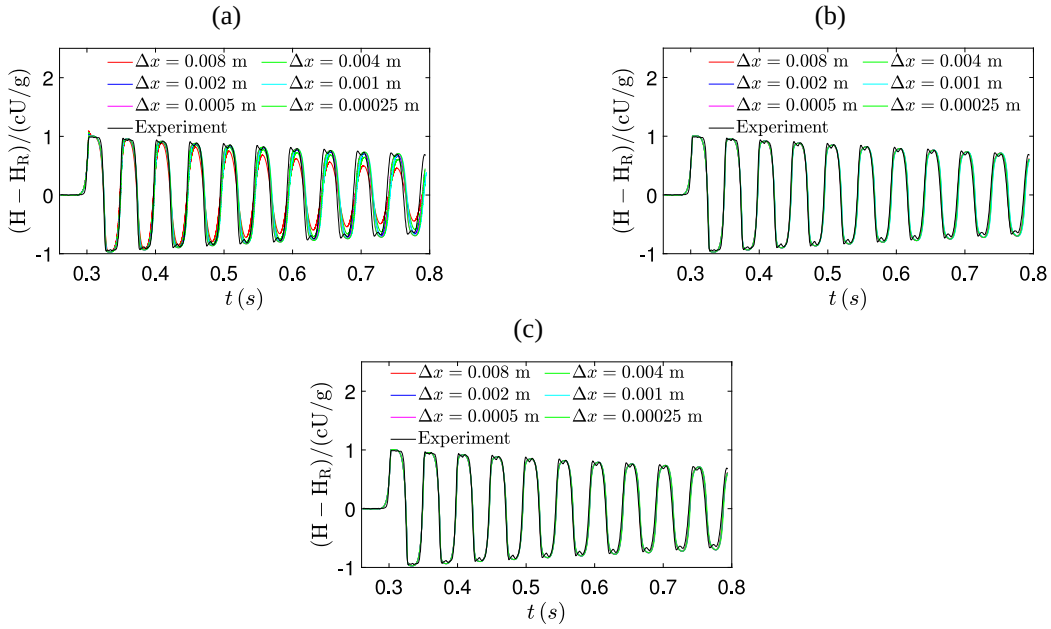

Figure 3. Obtained results by changing the Δx value. (a) SPH results with $\alpha = 2.0$. (b) MOC results, and (c) SPH results with $\alpha = 0.8$.

To ensure stability, the α value of the artificial viscosity was reduced to 0.8. That eliminated overshoot on the first peak without any pre-smoothing treatment and avoided any smearing effect in the SPH results shown in Fig. 3c. The L_2 error values for SPH results with $\alpha = 0.8$ remained around 0.350 for $\Delta x \leq 0.020$ m, and increased to 0.380 for for $\Delta x \geq 0.040$ m.

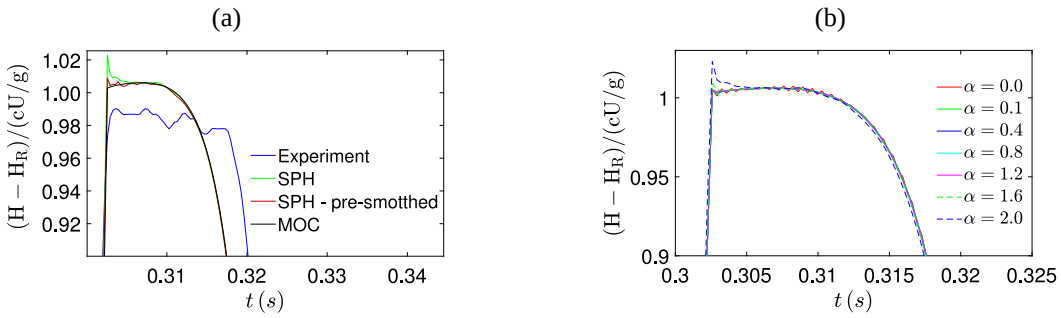

Figure 4. Analysis of the first pressure peak shows distinct overshoot due to dispersion errors. Pre-smoothing technique (a) and artificial viscosity (b) effects observed.

After examining Fig. 4b, it was found that artificial viscosity was necessary to prevent dispersion error in the initial peak. Adjusting the α value to 0.1 mitigated the dispersive errors, with only a slight overshoot on the pressure peak's left side. However, $\alpha \geq 1.6$ caused dispersive errors to resurface and increase. A high α value can

also cause pressure to smear, as observed when $\alpha = 2.0$, which resulted in a prominent smearing effect displayed in Fig. 3a. With an appropriately adjusted α, the SPH remains stable relative to the number of particles, but there was an offset from the experimental results, which may indicate the CSPH corrective equations are responsible.

There is a difference in running time of simulation between the SPH and MOC methods when using an Intel(R) Core(TM) i5-8265U CPU 1.60 GHz 1.8 GHz 12.0 GB RAM Windows x64. On average, the SPH method is 7% to 15% faster than the MOC method, Tab. 2.

Table 2. Running time of simulations in seconds for each numerical method.

	Δx (m)					
Methods	0.08	0.04	0.02	0.01	0.005	0.0025
SPH	4.556	17.740	72.025	281.380	1183.520	4433.690
MOC	5.404	19.093	84.534	310.852	1222.514	4707.004

7 Conclusions

The present study compares the SPH and MOC methods. An unsteady friction model is incorporated to account for the effects of friction on hydraulic transient phenomena. The findings reveal that while both methods initially align with experimental data, the SPH encounters difficulties during valve maneuvers and requires pre-smoothing techniques to reduce errors and eliminate smearing effects despite having advantages in computational efficiency. Additionally, SPH produces higher errors than MOC. The study emphasizes the importance of refining hydraulic transient modeling and highlights the role of artificial viscosity in achieving stability. Finally, it acknowledges the potential and challenges associated with SPH in simulating hydraulic transients.

Acknowledgements. The first author is grateful to PPGMEC program from the Federal University of Goiás (UFG) for the opportunity to study and for all the support.

Authorship statement. The authors hereby confirm that they are the sole liable persons responsible for the authorship of this work, and that all material that has been herein included as part of the present paper is either the property (and authorship) of the authors, or has the permission of the owners to be included here.

References

[1] A. E. Vardy, A. C. L. Chan, and W. G. Anderson. “A general model for water hammer with friction”. *Journal of Hydraulic Research*, vol. 5, n. 31, pp. 647–663, 1993.
[2] N. M. C. Martins, A. K. Soares, H. M. Ramos, and D. I. C. Covas. “Cfd modeling of transient flow in pressurized pipes". *Computer and Fluids*, vol. 126, pp. 129–140, 2016.
[3] E. B. Wylie and V. L. Streeter. *Fluid transients in systems*. Prentice Hall, 1993.
[4] B. Brunone, B. W. Karney, and B. W. Ferrante. “Method of characteristics solution of pipe system transients”. *Journal of Hydraulic Engineering*, 128 (3), pp. 282-289, 2002.
[5] M. H. Chaudhry. *Applied hydraulic transients*. Springer, 2014.
[6] M. S. Ghidaoui and S. Mansour. “Efficient Treatment of the Vardy–Brown Unsteady Shear in Pipe Transients”. *Journal of Hydraulic Engineering*, 128 (3), pp. 102-112. 2002.
[7] S. Chen, T. Belytschko, and J. Xu. “A simple and stable correction for sph with the sph particle-in-cell method”. *Computer Methods in Applied Mechanics and Engineering*, vol. 3-4, n. 173, pp. 315–330, 1999.
[8] J. J. Monaghan and R. A. Gingold. “Shock simulation by the particle method sph*”. Journal of Computational Physics*, vol. 2, n. 52, pp. 374–389, 1983.
[9] W. Zielke. “Frequency-dependent friction in transient pipe flow”. *Journal of Basic Engineering, Trans ASME*, vol. 90, pp. 109–115, 1968.
[10] J. J. Monaghan and J. C. Lattanzio. “A refined particle method for astrophysical problems”. *Astronomy and Astrophysics*, vol. 149, pp. 135–143, 1985.
[11] J. J. Monaghan. “On the problem of penetration in particle methods”. *Journal of Computational Physics*, vol. 82, pp. 1–15, 1989.
[12] Q. Hou, A.C.H. Kruisbrink, A.S. Tijsseling, and A. Keramat. “Simulating water hammer with corrective smoothed particle method”. *BHR Group - 11th International Conferences on Pressure Surges*, pp.171-187, 2012.